文章编号: 1001－2060(2007)06－0673－04

喷淋脱硫塔喷嘴外流动数值模拟与实验研究

周山明, 金保升, 孙志翱
(东南大学 洁净煤发电与燃烧教育部重点实验室, 江苏 南京 210096)

摘　要: 建立了一个喷淋脱硫塔喷嘴数值模型, 研究了影响喷淋脱硫塔内气液传质的喷淋液流量与液膜平均破裂长度、喷嘴初始喷射角、液滴平均粒径的关系。设计了专门的测试平台和单匝螺旋喷嘴, 采用快速 CCD 和数码照相机拍照对液膜和液滴运动进行了测试和分析。模型计算和实验结果均表明: 液膜平均破裂长度随喷淋液流量加大而减小; 液滴平均粒径减小随喷淋液流量加大而减小; 在喷嘴出口缝隙高度等于 4.25 mm 时, 随流量的增大, 喷嘴的喷射角随流量的增大反而变小, 大于 4.25 mm 后, 在同一喷嘴缝隙高度下, 喷射角随喷嘴流量的增加而增加。

关　键　词: 液膜模型; 破裂; 喷射角; 平均粒径
中图分类号: X701.3　　文献标识码: A

符 号 说 明

b_0—喷嘴出口处液膜厚度;
b—液膜厚度;
C—积分常数;
d_L—液丝(条)直径;
d_D—液滴直径;
g—重力加速度;
h—喷嘴出口高度;
L—液膜破碎长度;
n—液滴数;
Oh—准则数;
P—压力;
P_∞—空气压力;
R—液膜外边界;
R_0—喷嘴出口处外边界;
R_1—液膜内边界;
r—径向直径;
T_c—由表面张力引起的从液膜表面向液膜内部渗透的扰动长度;
T_v—由粘性作用引起的从液膜表面向液膜内部渗透的扰动长度;
$\vec{U}$—液膜中液体速度向量;
U—气液相对速度;
u—径向速度;
u_R—液膜外边界径向速度;
V_L—液丝体积;
w—轴向速度;
z—垂直高度;
θ—周向角度;
μ—液体粘性系数;
ν—液体动力粘度;
ρ_G—空气密度;
ρ_L—液体密度;
σ—液体表面张力

引　言

在大型烟气脱硫装置中, 目前绝大部分均使用了喷淋方式脱硫。采用喷淋方式可以有较大的气液接触比, 对烟气的阻力较小, 同时由于没有转动部件, 设备的维修期很长。

而在喷淋脱硫中, 喷嘴对脱硫的过程有着十分重要的影响。喷嘴对塔内浆液的分布和浆液粒径大小的控制至关重要, 这些参数的改变可使脱硫塔内气液接触面积和气液接触效果产生很大差异, 因此对喷嘴的流动进行研究在喷淋式烟气脱硫中有十分重要的意义。

许多研究者对喷嘴和线性非稳态液膜的流动状况进行了研究, 详细考察了液膜周围气流、液体的粘性、液体的表面张力等对液膜流动及破裂的影响, 并提出了液膜破裂后液滴的平均直径计算关联式[1~3]。在液膜的流动过程中, 外界对液膜的扰动以波的形式在液膜中扩散, 随着液膜的流动, 这种扰动形成波不断增强, 而液膜在液体粘性力、表面张力、重力以及外界扰动形成波的作用下, 液膜表面将产生晃动, 而晃动的幅度随着液膜的流动过程中不断变大, 当其幅度超过一定程度后, 液膜将破裂形成液丝, 液丝在液体表面张力的作用下形成液滴[4~5]。文献[6]对粘性液体在高速流动下形成的液膜进行了研究, 推导出了长波扰动和短波扰动下波的复杂增长率 ω 的理论公式和液膜破裂长度 L 和液滴的粒径 d_D。文献[7]对压力旋流喷嘴流动雾化进行了数值模拟, 其模拟结果与实验值吻合很好。国内学者则主要研究喷嘴雾化情况及颗粒粒径分布等, 并提出了相应的实验关联式[8~9], 对喷嘴出口处液膜的运动及破裂则少有文献报道。

在前人的研究基础上, 本文建立一个针对脱硫喷淋塔中实用喷嘴的流动数值模型, 并通过实验来验证模型的准确性。

1　模型

1.1　喷嘴内部流场计算

模型中对喷嘴的内部流场计算采用了 $k-\varepsilon$ 方程, 计算是在商业软件 Fluent 界面下进行的, 计算基

收稿日期: 2007－01－04;　修订日期: 2007－04－12
基金项目: 国家重点基础研究发展规划基金资助项目(G19990221053)
作者简介: 周山明(1969－), 男, 江西萍乡人, 东南大学讲师, 博士研究生。

于紊流 $k-\varepsilon$ 模型，采用结构化网格，进口采用质量流量，出口设为压力界面。喷嘴内部网格数均大于 100 万，一个工况计算时间约 10 h。计算出喷嘴出口速度分布作为液膜起始参数。

1.2 液膜边界（R、R_1）

液膜的形状示意图及坐标系统如图 1 所示。

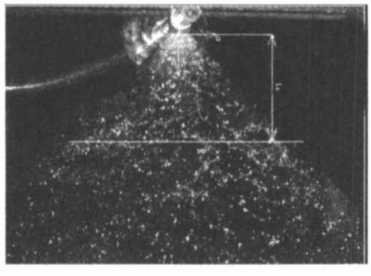

图 1 液膜形状、坐标系统及破裂长度示意图

在本模型中，对液膜的流动作以下假设：

（1）定常流；（2）$\partial v/\partial\varphi=0$；（3）$\partial\vec{U}/\partial\theta=0$；（4）忽略烟气对液膜的流动阻力。

浆液流动的连续性方程：

$$\frac{\partial}{r\partial\varphi}(ur)+\frac{\partial w}{\partial z}=0 \tag{1}$$

Z 向动量方程：

$$w\frac{\partial w}{\partial z}=-\frac{\partial P}{\rho\partial z}+g+2v\frac{\partial^2 w}{\partial z^2}+\frac{v\partial}{r\partial\varphi}\left(r\frac{\partial u}{\partial z}\right) \tag{2}$$

由式(1)及假设(2)可解得：

$$ur=-\frac{r^2}{2}\frac{\partial w}{\partial z}+C \tag{3}$$

对于液膜外径则有：

$$u_R=\frac{\mathrm{d}R}{\mathrm{d}t}=\frac{\mathrm{d}R}{\mathrm{d}z}\frac{\mathrm{d}z}{\mathrm{d}t}=w\frac{\mathrm{d}R}{\mathrm{d}z} \tag{4}$$

在液膜边界处有：

$$P-\frac{\tau_R}{2}=P_\infty+\frac{\sigma}{R} \tag{5}$$

$$\tau_r=2\mu\frac{\partial u}{\partial r} \tag{6}$$

假设 P_∞=常数，整理式(1)~式(6)，则有：

$$w\frac{\partial w}{\partial z}=g+2v\frac{\partial^2 w}{\partial z^2}+\frac{\sigma}{\rho R^2}\frac{\partial R}{\partial z}-C\frac{\partial r}{\partial z}-\frac{1}{2}\frac{\partial w}{\partial z}\frac{\partial r}{\partial z} \tag{7}$$

对于液膜边界，则有：

$$w\frac{\partial w}{\partial z}=g+2v\frac{\partial^2 w}{\partial z^2}+\left(\frac{\sigma-\rho C}{\rho R^2}-\frac{1}{2}\frac{\partial w}{\partial z}\right)\frac{\partial R}{\partial z} \tag{8}$$

联立式(1)、式(4)和式(8)可求出液膜外边界 R。对于液膜内径，有：

$$w_0\pi(R_0^2-(R_0-b_0)^2)=w_0\pi(R^2-(R-b)^2)w_0$$

其中：$b=R-R_1$，则：

$$R_1=\sqrt{R^2-\frac{w_0(R_0^2-(R_0-b_0)^2)}{w}} \tag{9}$$

1.3 液膜破碎

文献[1, 10]提出两个“渗透厚度”（扰动长度）概念，即：

$$T_c=(\rho_g U^2/\sigma)^{-1} \tag{10}$$

$$T_v=(\rho_l U/\mu)^{-1} \tag{11}$$

其中：T_c—由表面张力引起的从液体表面向液体内部渗透的扰动长度；而 T_v—由表面粘性作用引起的从液体表面向内部传播的扰动长度，当液膜厚度远大于 MAX（T_c, T_v）时，液膜不易破裂，而当 $b<$MAX（T_c, T_v）时，液膜扰动变得很强烈，因而易于破裂。由此可知，MAX（T_c, T_v）可以作为判别破裂的一个准则数。在本模型中，根据实验数据，取 $b/4=$MAX（T_v, T_c）为液膜破裂标准。

1.4 液滴粒径

根据线性稳态理论，液膜破碎后首先形成丝带状，这些丝带状的液条在表面张力和外力作用下再裂解成液滴。文献[6]利用线性稳态理论推导出液条直径表示式：

$$d_L=(16h\sigma/\rho_g)^{0.5}/U \tag{12}$$

而由其形成的液滴粒径则为：

$$d_D=1.88d_L(1+3Oh)^{0.1667} \tag{13}$$

$$Oh=\mu_L/(\rho_L\sigma d_L)^{0.5} \tag{14}$$

假设液膜破裂成圆环状液条，则液条体积可由下式计算：

$$V_L=2\pi^2(R-b/2)d_L^2/4 \tag{15}$$

则单条液丝产生的液滴数为：

$$n=6V_L/(\pi d_D^3) \tag{16}$$

计算是在 Matlab 界面下进行的，采用一台 Pentium4 处理器主频 3.0 GHz 的计算机进行计算，一个工况需计算 7 mis 左右。

2 实验装置与参数

实验参数如表 1 所示。图 2 为实验装置示意图，由水箱、水泵、流量计、水管及喷嘴构成循环体系，另有一旁通管构成稳压回路，平衡由于水泵压力波动造成的流量的波动。图 3 为喷嘴结构示意图，其内径为 20 mm，在喷嘴下部设置一个圆台，圆台与置于喷嘴中央的螺杆相连用来调节喷嘴出口缝隙高度。喷嘴连同导管被固定于一个水槽上部一定高度，采用一台日本 Photron 公司的快速 CCD（型号为：FASTCAM-NET-MAX3）以及一台数码相机（OLYMPUS C5060）对喷嘴进行拍照和摄像，从而获取实验图象，

对图像进行灰度对比处理后可以获得实验数据。

表 1　实验参数表

	数值			
实验温度/ ℃	20			
水密度/kg·m^{-3}	998			
空气密度/kg·m^{-3}	1.293			
水粘度/kg(m·s)$^{-1}$	1.79× 10^{-5}			
水表面张力/N·m^{-1}	0.072			
空气流速/m·s^{-1}	0.5~1.0			
水流量/t·h^{-1}	5	6.5	7	7.7
喷嘴缝隙高度 h/mm	4.25	5	6	6.5

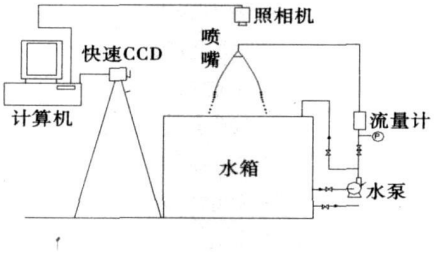

图 2　实验装置示意图

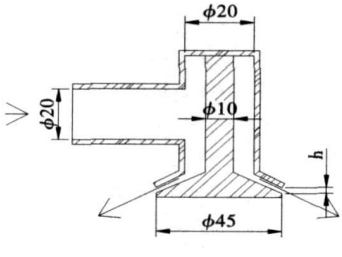

h—喷嘴出口缝隙高度

图 3　单匝喷嘴示意图

3　结果与讨论

实验发现, 喷嘴液体喷射呈垂直轴对称状态, 但在喷嘴进口导管的下方喷嘴出口处, 其液膜形状有明显的下凹, 这是由于喷嘴进口导管的位置不在垂直轴上, 使喷嘴内部的液体流动不均匀影响到喷嘴出口处的速度分布, 进而影响了液膜的形态而不能形成周向对称。但由于其范围较小, 且难于测量, 在本文中忽略了这种差别。由于设备原因, 图象采集速度最高只能达到 500 帧/s, 因此测量液滴的粒径由于运动原因而产生误差, 实验中测量液滴的在运动方向上呈线状。在后期数据处理中, 将照片的曝光时间和运动速度作为修正液滴粒径的因素, 每次实验在照片上随即取 50 个液滴的粒径均值作为此次实验液滴平均粒径。

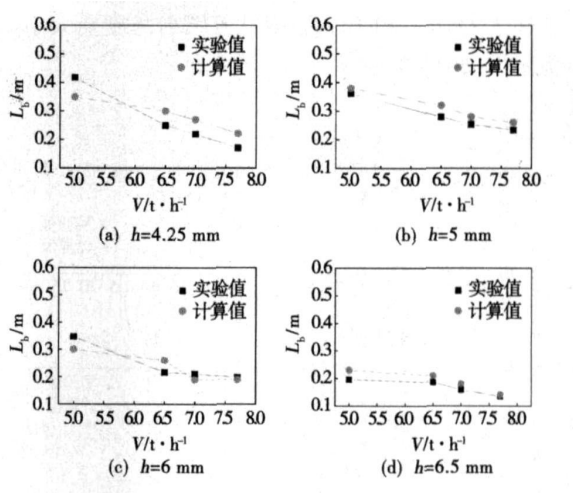

图 4　液膜破裂与流量关系图

图 4 为在不同喷嘴出口缝隙高度下液膜破裂长度与流量关系图。此处液膜平均破裂长度定义为从喷嘴出口到可见大量分散相液滴的垂直距离。由图可知, 液膜破裂长度随流量的增大而减小。随着流量的增加, 液体出口平均速度增大, 气液相对速度 U 也随之增加, 此时液膜内部流动处于紊流状态, 外界对其扰动将以更快的速度在液膜内进行传播, 从而加剧了液膜内部的扰动, 而液膜内部的扰动加大则使液膜的稳定性变弱, 这将导致液膜在大流量下的破碎长度变短; 另一方面, 喷嘴出口流量增大可使喷嘴出口处液体的初速度增加, 从而使液膜具有较大的扩展能力, 但这种扩展趋势与由于扰动引起的液膜维持能力变弱的趋势相比要小得多, 因此总体上表现为随流量的增加液膜的平均破裂长度变小。文献[11] 液膜破裂长度实验结果也与本模型的预测结果趋势一致。

图 5 为喷射角与喷嘴流量关系图。此处的喷射角为液膜与垂直轴的夹角, 由于液膜在出口后并不是沿直线行进, 本文中的喷射角指出口处液膜与垂直轴的夹角。由图可见, 在喷嘴出口缝隙高度大于 4.25 mm 后, 在同一喷嘴缝隙高度下, 喷射角随喷嘴流量的增加而增加, 当喷射流量加大后, 液体的出口动能变大, 在径向抵御重力的引起的速度方向改变的能力也随之变大, 因此喷射角也随之增大。而在图 5(a)中可见, 当喷嘴出口缝隙高度为 4.25 mm, 随流量的增大, 喷嘴的喷射角随流量的增大反而变小, 这与喷嘴出口处液膜厚度和喷嘴出口速度分布有关。从计算出口速度分布中可以看出: 靠近喷嘴底部的速度方向改变是液膜喷射角改变的主要因素, 在小流量下, 靠近喷嘴底部的流量占总流量的比例

要高于大流量下的比例，因此其喷射角度要大于大流量下的喷射角度。

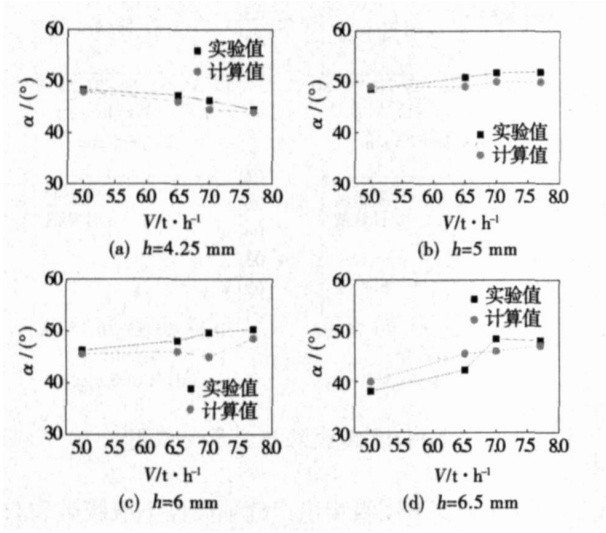

图 5 喷射角与流量关系图

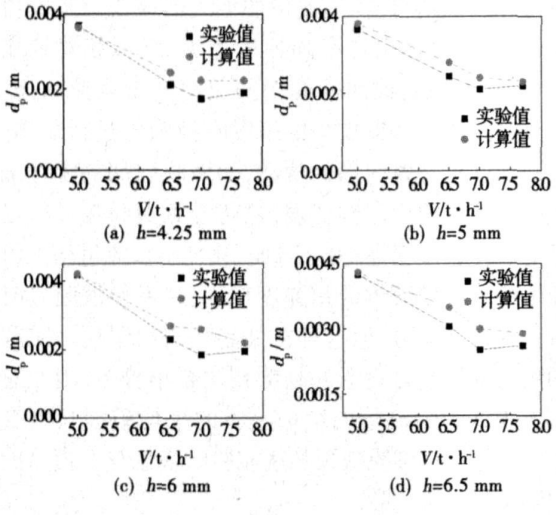

图 6 液滴平均直径与流量关系图

图 6 为液滴平均直径与流量关系图。由图可见，对于任一喷嘴出口缝隙高度，液滴的平均粒径变化随流量改变的趋势相同，流量增大时，液滴的平均粒径减小，但流量增加到一定量时，生成的液滴粒径却有所增大。当喷嘴出口流量加大后，液体的平均出口速度也增大，由液膜表面张力和表面粘性作用引起的“渗透厚度”随之变小，即干扰波波长变短。根据液膜波动理论，液膜破裂发生在半波处，当干扰波波长变短后，液膜破裂后形成的液丝直径也变小，由此引起的液滴直径变小。但当出口流量继续变大时，由液膜表面张力和表面粘性作用引起的“渗透厚度”变得很小，此时液膜的破裂可能发生在全波长处甚至几个波长处，此时表现为液滴粒径就有可能增加或保持不变。由于在后期数据处理中采用的是出口平均速度为补偿速度，这种补偿速度要低于液滴的当地速度，因此图 6 中实验值均比对应的计算值要高。

4 结 论

采用简化 $N-S$ 方程并引入“渗透厚度”作为液膜破裂标准来模拟液膜流动状况，进而对破裂后形成液滴的颗粒的平均粒径进行预测，取得了很好的效果，与实验结果吻合较好。通过模型计算和实验研究可得出以下结论：

（1）在大流量低压力条件下，通过喷嘴的流量越大，液膜的平均破裂长度越小；

（2）在喷嘴出口大缝隙高度条件下，喷射角随流量的增加而增加，但在小缝隙高度条件下，喷射角随流量增加反而有细微的减小；

（3）液滴粒径随流量的增加而减小，但减小趋势随流量的增大而减小；

（4）在低压力大流量喷嘴流动中，由液膜表面张力和表面粘性作用对液膜破裂影响有决定作用。

参考文献：

[1] SQUIRE H B. Investigation of the instability of a moving liquid film [J]. Brit J Appl Phys, 1953, 4: 167—169.

[2] HAGERTY W W, SHEA J F. A study of the stability of plane liquid sheets[J]. J Appl Mech, 1955, 22: 509—514.

[3] SHEN J, LI X. Atomization of an annular viscous liquid jet //Proc 7th Annu Conf Liquid Atom[C]. Spray Sys: ILASS, North and South America, 1994. 50—54.

[4] TAYLOR G. The dynamics of thin sheets of fluid disintegration of fluid sheets[C]. Proc Roy Soc, 1959, 253, 313.

[5] DOMBROWSKI N. The aerodynamic instability and disintegration of viscous liquid sheets[J]. Chem Eng Sci, 1963, 18, 203.

[6] SENECAL P K, SCHMIDT D P, NOUAR I, et al. Modeling high-speed viscous liquid sheet atomization[J]. International Journal of Multiphase Flow, 1999, 25: 1073—1097.

[7] NONNENMACHER S, PIESCHE M. Desigh of hollow cone pressure swirl nozzles to atomize newtonian fluids[J]. Chemical Engineering Science, 2000, 55: 4339—4348.

[8] 刘乃玲，张 旭. 压力式螺旋型喷嘴雾化特性实验研究[J]. 热能动力工程，2006，21(5)：505—507.

[9] 王乃华，高 翔，骆仲泱，等. 石灰浆液雾化喷嘴及其特性研究[J]. 热能动力工程，2001，16(5)：247—249，254.

[10] RAYLEIGH L. On the instability of jets[J]. Proc London Math Soc, 1879, 10(4): 351—371.

[11] SHMIDT D P, NOUAR I, SENECAL P K, et al. Pressure-swirl atomization in near field[J]. International Journal of multiphaxe flow, 1999, 25: 1073—1097.

（编辑 柴 舒）

certainty range of the output of an on-line performance calculation model for plants under different outside boundary conditions, different operating parameters as well as identical operating conditions, thus providing useful reference data for optimization decision-making adjustment and diagnosis both based on the model in question. The coal consumption characteristic curves of the plant obtained through statistical calculations reflect the actual characteristics of the plant under real operating conditions. With the in-plant load distribution version serving as an example, the effectiveness of the measures taken for economic operation has been verified. **Key words**: thermal power plant, on-line performance calculation, statistical characteristics, uncertainty, load distribution

电站锅炉温室气体排放量的计算＝**Calculation of Greenhouse Gas Emissions from Utility Boilers**[刊, 汉] /LIU Huan-zhang, CHANG Tai-hua, LIU Ji-zhen, et al (Automation Department, North China Electric Power University, Beijing, China, Post Code: 102206)// Journal of Engineering for Thermal Energy & Power. — 2007, 22(6). —665 ~ 668

As an important secondary energy source, electric power is indispensable. However, a large quantity of waste emissions is produced during power generation, especially by coal-fired power plants. On the basis of flue gas analysis, a study of fuel characteristic coefficients and by analyzing combustion mechanism as well as through a modeling based on statistical laws, a forecast was given of the greenhouse gas carbon-dioxide emissions from coal-fired utility boilers. Finally, a simulation study was conducted of the forecasting method by making use of the real-time historic data from Panshan Power Plant. The simulation indicates the feasibility of the method under discussion. **Key words**: flue gas analysis, fuel characteristic coefficient, utility boiler, greenhouse gas

石灰石脱硫反应对喷氨脱硝反应影响的实验研究＝**An Experimental Study of the Effect of Limestone Desulfurization Reaction on Ammonia-injected Denitrification Reaction**[刊, 汉] /HOU Xiang-song, WANG Jin-wei, ZHANG Hai, et al (Education Ministry Key Laboratory on Thermal Science and Power Engineering, Thermal Energy Engineering Department, Tsinghua University, Beijing, China, Post Code: 100084)// Journal of Engineering for Thermal Energy & Power. — 2007, 22(6). —669 ~ 672

To inject ammonia into a CFB (circulating fluidized bed) boiler at its furnace tail portion or at the inlet of a cyclone separator can reduce the NO_x content in flue gases. In a CFB boiler, the injection of limestone for the purpose of desulfuration may influence the ammonia-injected denitrification reaction. An experimental study was conducted of the impact of pyrolytic and desulfuration products of the limestone on ammonia-injected denitrification reaction. It has been found that the pyrolytic reaction products of limestone prior to desulfuration have a relatively big specific surface area and CaO exhibits a definite catalytic activity, which can promote the ammonia-injected denitrification reaction. The desulfuration products of the limestone exercise a relatively small influence on the ammonia-injected denitrification reaction. When the temperature is above 1 200 K, however, the products in question can promote the oxidation of NH_3 and reduce the escape of NH_3, both aspects being considered as favorable to the ammonia-injected denitrification reaction. **Key words**: circulating fluidized bed, ammonia-sprayed denitrification, limestone, catalysis

喷淋脱硫塔喷嘴外流动数值模拟与实验研究＝**Numerical Simulation and Experimental Study of Flows Outside the Nozzles of a Spray-type Desulfuration Tower**[刊, 汉] /ZHOU Shan-ming, JIN Bao-sheng, SUN Zhi-ao (Education Ministry Key Laboratory on Clean Coal Power Generation and Combustion Technology, Southeast University, Nanjing, China, Post Code: 210096)// Journal of Engineering for Thermal Energy & Power. —2007, 22(6). —673 ~ 676

Established was a numerical simulation model for nozzles of a spray-type desulfuration tower and studied was the relationship among the following items, which can influence the gas-liquid mass transfer inside a spray type desulfuration tower: spray liquid flow rate, average rupture length of the liquid film, initial jet flow angle of the nozzle and average liquid drop diameter. A special test platform and single-turn spiral nozzle were designed and the liquid film and liquid-drop movement were tested and analyzed by using a quick-speed CCD (Charge Coupled Device) with a digital camera being used to take pictures. Both the model calculations and experimental results show that the average liquid film rupture-length and the average liquid drop diameter will decrease with an increase of spray liquid flow rate. When the clearance height at the nozzle

outlet is 4.25 mm, the spray angle of the nozzle will decrease with an increase of the liquid flow rate and when the clearance height at the nozzle outlet is greater than 4.25 mm, the spray angle under a same nozzle clearance height will increase with an increase of the liquid flow rate. **Key words**: spray type desulfuration tower nozzle, liquid film model, rupture, spray angle, average particle diameter

湿法烟气脱硫对锅炉稳定运行的影响与对策分析= **Effect of Wet-method Flue Gas Desulfurization on Boiler Stable Operation and Analysis of Related Countermeasures**[刊, 汉] / LI Da-zhong, ZHANG Rui-xiang (Automation Department, North China Electric Power University, Baoding, China, Post Code: 071000), SHUAI Guo-qiang (Guohua Dingzhou Power Generation Co. Ltd, Dingzhou, China, Post Code: 073000)// Journal of Engineering for Thermal Energy & Power. — 2007, 22(6). —677 ~680

The use of flue gas desulfurization (FGD) in power plants is one of the effective measures to reduce SO_2 emissions, among which limestone/plaster wet method desulfurization technology is the most proven one. However, in the FGD system, such problems as unreliability of the supercharged fan control system and a blockage in a gas-gas heater (GGH) have brought about many adverse effects to boiler stable operation. In practical applications, it is possible to open a bypass baffle in the desulfurization system and change the control mode to enhance the stability of boiler flue gas and air system. Measures, such as improving the GGH on-line wash mode etc. may be taken to effectively control the blockage. With Dingzhou Power Plant serving as an example, an in-depth analysis and study was conducted to seek solutions to the above problems. **Key words**: wet-method flue gas desulfuration, boiler stable operation, analysis of countermeasures

液相生化法烟气脱硫实验研究= **Experimental Study of Flue Gas Desulfuration by Using a Liquid-Phase Biochemical Method**[刊, 汉] / LIU Qi-wang, LIU Zhi-an, ZHANG Zhi-jian (College of Energy Source and Power Engineering, Inner Mongolia University of Technology, Huhhot, China, Post Code: 010051), ZHANG Chun-feng (Chemical Engineering College, Inner Mongolia University of Technology, Huhhot, China, Post Code: 010051)// Journal of Engineering for Thermal Energy & Power. — 2007, 22(6). —681 ~683

By combining the transition metal (Fe^{3+}/Fe^{2+} galvanic couple) catalytic oxidation with microbic metabolism function and making use of the strong oxidation of iron ion Fe^{3+}, S(Ⅳ) can be oxidized to S(Ⅵ) with the iron ion Fe^{3+} being reduced to Fe^{2+} while the microbe (hereinafter referred to as DYB1 for short) metabolism function can be used to quickly convert Fe^{2+} to Fe^{3+}. By a synergism of the latter two a desulfuration cycle can be completed. An indoor experiment was performed under the following parameter conditions: liquid/gas ratio, 2.70 ~8.40 L/m^3, amount of ash conveyed, 16 ~30 g/min, wind speed inside the turbulence ball tower, 4 ~15 m/s, concentration of iron ion, 1.60 ~3.00 g/L (calculated on the basis of Fe_2O_3), pH value, 2.7 ~5.0, concentration of SO_2, 2574 ~5434 mg/m^3. The test results show that the concentration of Fe^{3+} plays an obvious role of controlling the reaction and the products generated Fe^{2+} and SO_4^{2-} exercise an inhibitive role to the reaction, especially Fe^{2+}, because the latter can react with HSO_3^- to produce an internal complex and affect the generation of $SO_3^{\cdot-}$ free radical, putting an end to the reduction reaction of oxidization. After DYB1 has been added, Fe^{2+} can be effectively converted to Fe^{3+}, enabling the above-cited reduction reaction of oxidization to sustain and continue. The desulfuration rate can be 19 ~49 percentage points higher than that under same conditions and when no DYB1 has been added. **Key words**: liquid-phase biochemical method, flue gas desulfuration, experimental study